



Heavy Ions Radiation Effects on 4kb Phase-Change Memory

Anna Lisa Serra, Tobias Vogel, Gauthier Lefevre, Stefan Petzold, Nico Kaiser,
Guillaume Bourgeois, Marie-Claire Cyrille, Lambert Alff, Christina
Trautmann, Christophe Vallée, et al.

► To cite this version:

Anna Lisa Serra, Tobias Vogel, Gauthier Lefevre, Stefan Petzold, Nico Kaiser, et al.. Heavy Ions Radiation Effects on 4kb Phase-Change Memory. NSREC 2020 - Nuclear and Space Radiation Effects Conference, Dec 2020, Virtual Event, United States. cea-03086369

HAL Id: cea-03086369

<https://cea.hal.science/cea-03086369>

Submitted on 22 Dec 2020

HAL is a multi-disciplinary open access archive for the deposit and dissemination of scientific research documents, whether they are published or not. The documents may come from teaching and research institutions in France or abroad, or from public or private research centers.

L'archive ouverte pluridisciplinaire **HAL**, est destinée au dépôt et à la diffusion de documents scientifiques de niveau recherche, publiés ou non, émanant des établissements d'enseignement et de recherche français ou étrangers, des laboratoires publics ou privés.

Phase-Change Memory

Based on *Phase-Change Materials*:

Ex: $\text{Ge}_2\text{Sb}_2\text{Te}_5$ (GST), GeTe, etc.

- **Amorphous phase (logic state 0, RESET)**
- **Crystalline phase (logic state 1, SET)**

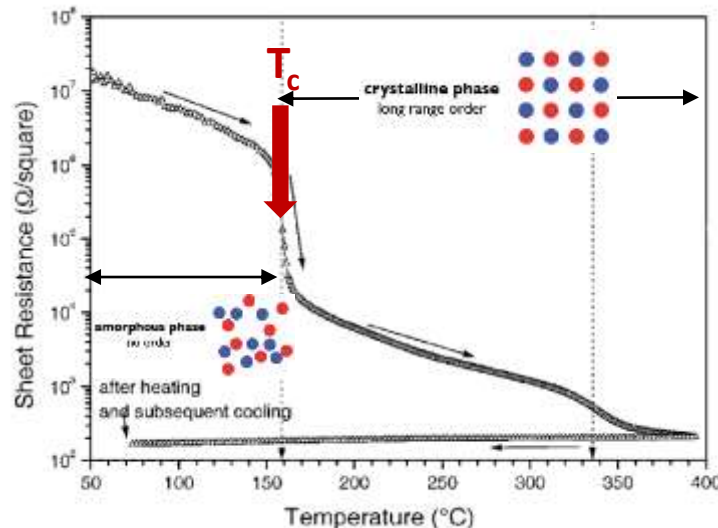


Fig.1 Resistivity as a function of temperature of a Phase-Change Material [1]

Memory programming relies on temperature profile control and not on charge storage

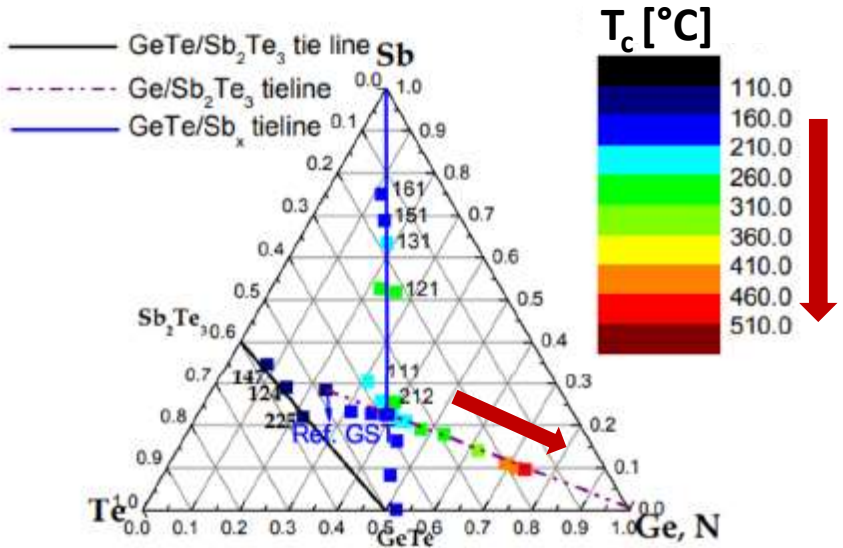


Fig.2 Crystallization temperatures T_c as a function of compositions in the Ge-Sb-Te ternary phase diagram [2]

The crystallization temperature (T_c) can be tuned by engineering the material composition (Ge or N enrichment)

[1] W. K. Njoroge, 2002

[2] H. Y. Cheng, 2012

PCM & radiation hardness

Radiation effects on the external circuitry

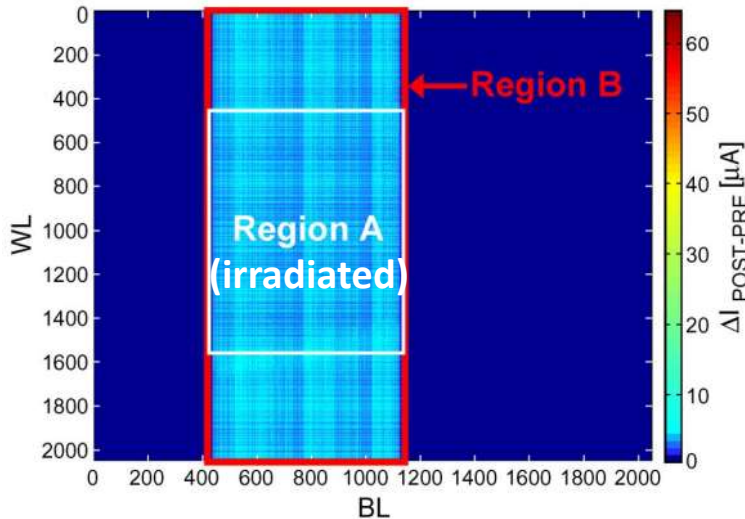


Fig. 3 Color map of the value of the cells of a MOS-chip array irradiated with a 30 Mrad SiO₂ proton beam. Region A is the irradiated zone and Region B is the area where the cells show a change in current of more than 1 A with respect to the pre-irradiation condition [3].

Devices belonging to the same WL or BL are affected by radiation, even if they do not lie in the irradiated region

Radiation effects on scaled PCM

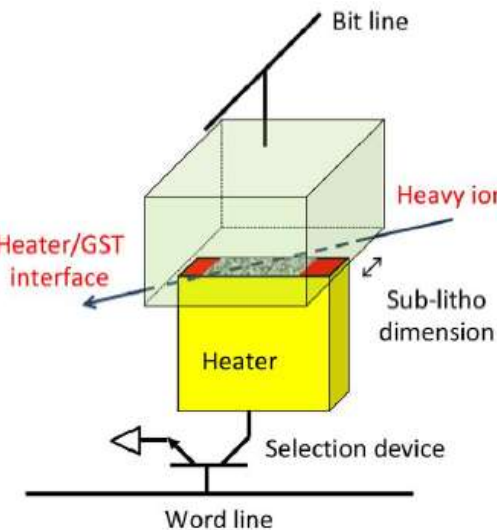


Fig. 4 Schematic of a phase change memory device hit by a heavy ion along the word line [4].

Partial amorphisation due to the temperature increase generated by the heavy-ions impinging on the active layer of 45 nm PCM

Radiation effect could impact the PCM depending on its device structure

Radiation effect on chalcogenide materials

GST and Ge-rich GeSbTe (GGST)

1. As deposited (amorphous)
 2. Annealed at 450°C (polycrystalline)
1. GST vs Ge-rich GeSbTe ($w=100\text{nm}$)
 2. GST vs Interfacial Layer-PCM ($w=300\text{nm}$)

Radiation effect on 4kb matrices

SET and RESET distribution

Irradiation beam specifications

- 8.3 MeV/u Au^{26+} -ions ($E=1.635 \text{ GeV}$)
- Flux: $5\text{E}8 \text{ ions/cm}^2 \text{ sec}$
- Fluences:
 $10\text{E}9, 5\text{E}10, 10\text{E}12, 5\text{E}12, 7\text{E}12,$
 $1\text{E}13 \text{ ions/cm}^2$
- Fluences :
 $10\text{E}9, 5\text{E}10, 10\text{E}12 \text{ ions/cm}^2$

GST vs GGST

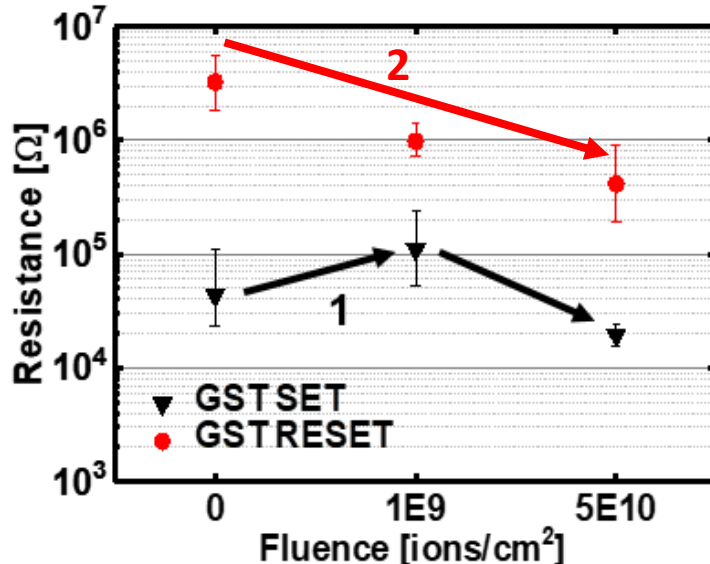


Fig. 5 Median and $\pm\sigma$ for SET and RESET distributions in GST 4kb arrays before and after irradiations at increasing fluences.

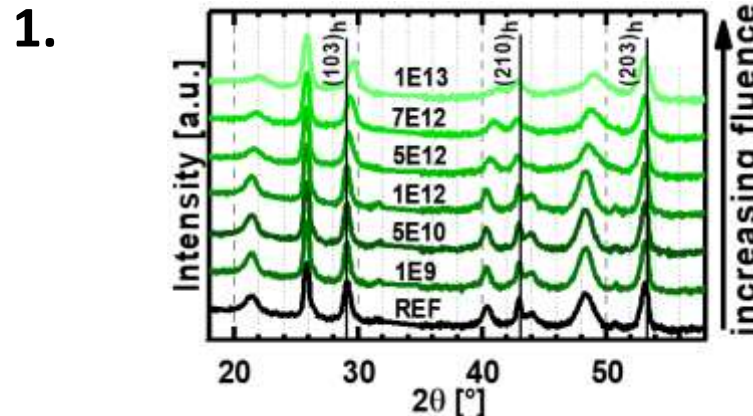


Fig. 6 XRD patterns of GST crystalline layers before (REF) and after irradiations at increasing fluence.

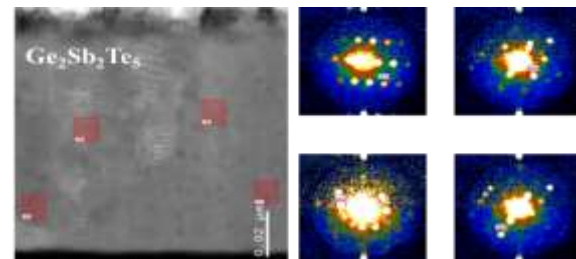


Fig. 7 TEM (left) and nano-diffraction patterns (right) analyses of as-deposited amorphous GST after irradiation at a fluence of 10^{13} ions/cm².

1. The SET state in GST faces a **structural relaxation** at a fluence of 10^{10} ions/cm² plus amorphisation at $5e10$ ions/cm²
2. The GST RESET resistance decreases with increasing fluence

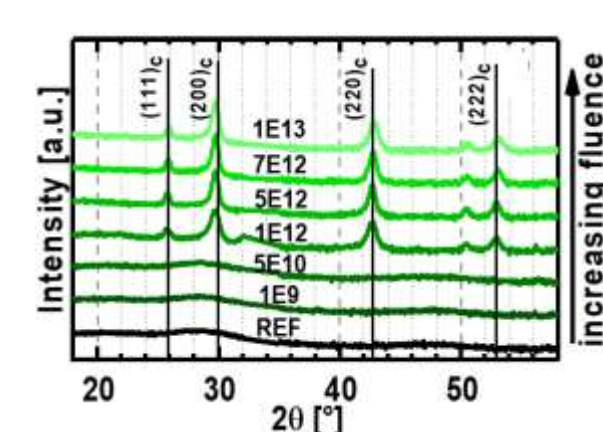


Fig. 8 XRD patterns of GST amorphous layers before (REF) and after irradiations at increasing fluence.

GST vs GGST

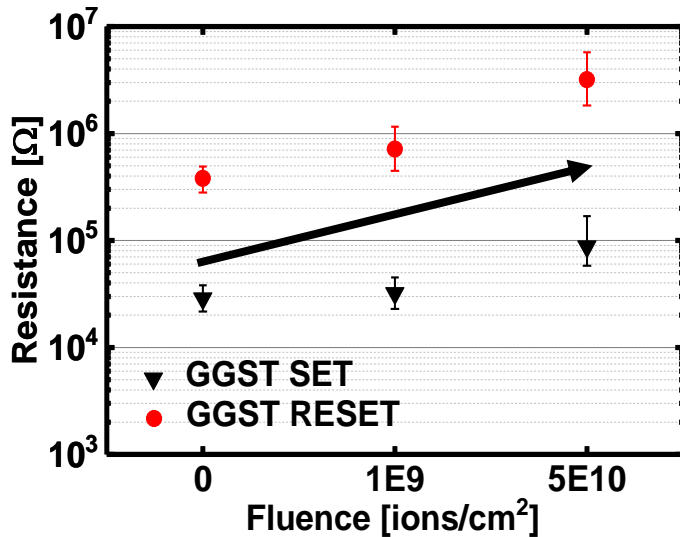


Fig. 9 Median and $\pm\sigma$ for SET and RESET distributions in GGST 4kb arrays before and after irradiations at increasing fluences.

SET and RESET states in GGST show structural relaxation at both fluences

Both the resistance window and the amorphous phase in the RESET state are preserved making GGST more stable than GST based devices thanks to its higher T_c

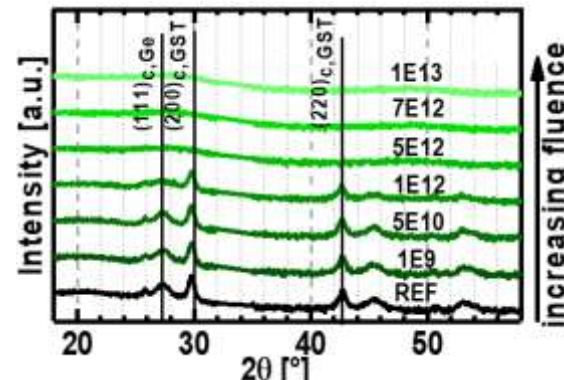


Fig 10 XRD patterns of GGST crystalline layers before (REF) and after irradiations at increasing fluence.

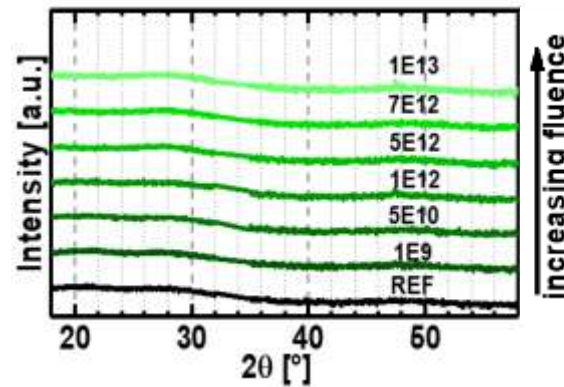


Fig 11 XRD patterns of GGST amorphous layers before (REF) and after irradiations at increasing fluence.

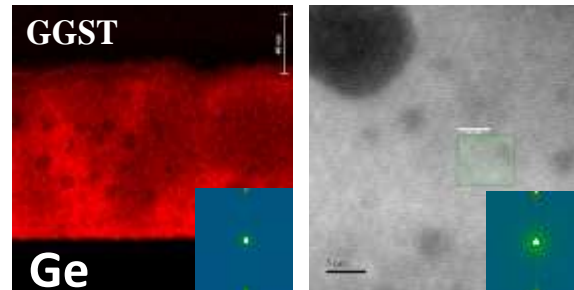


Fig 12 TEM/EDX and nano-diffraction patterns analyses of crystalline GGST after irradiation at a fluence of 7×10^{12} ions/cm². The Ge cartography (left) shows that the Ge segregation induced by the annealing process remains unchanged after irradiation. However, the irradiation reduces the size of the crystallites as evidenced by few and low intensity nano-diffraction patterns identified (right).

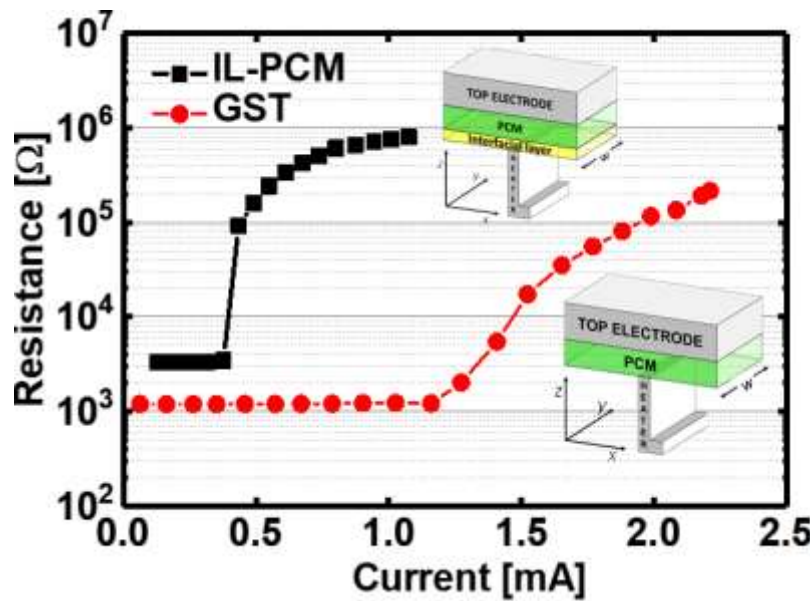


Fig. 13 Resistance-vs-Current characteristics comparing a standard GST device with an IL-PCM. IL-PCM shows a high current reduction wrt GST in devices featuring same critical dimension (electrode area $\sim 3 \times 10^{-3} \mu\text{m}^2$).

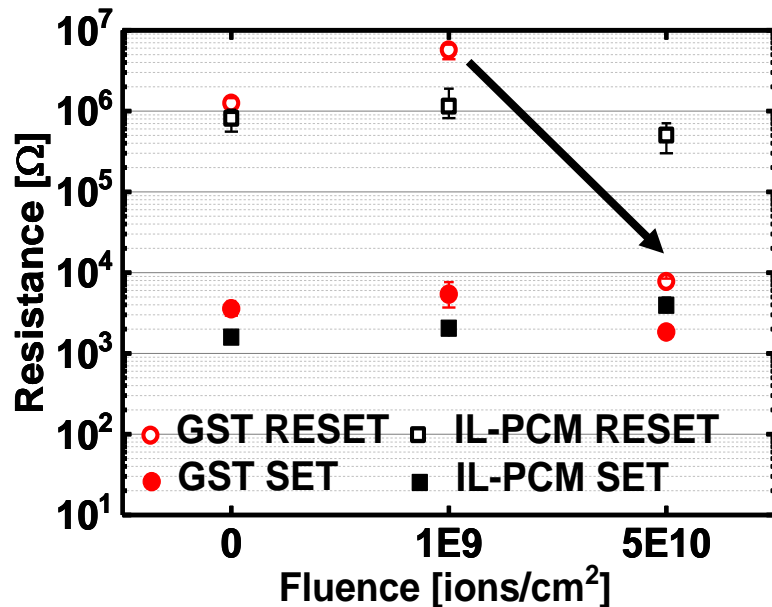


Fig. 14 Median and $\pm\sigma$ for SET and RESET distributions in GST and IL-PCM 4kb arrays before and after irradiations at increasing fluences.

GST vs IL-PCM

- Strong reduction in RESET current for IL-PCM wrt GST
- The higher SET resistance in IL-PCM is an evidence of the smaller contact area created during the programming of the cell

IL-PCM shows a higher radiation tolerance due to the « smaller » contact area between heater and PCM

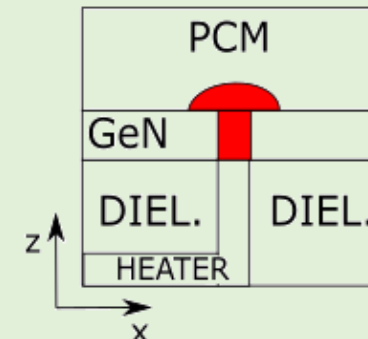


Fig. 15 Schematic of the zx-plane of an IL-PCM showing in red the programmed region, demonstrating the contact area reduction.